

Compact Dual-Band E-Shape Patch Antenna with Defected Ground Structure for 5G Millimeter-Wave Applications

D. Gh. Hammood¹, M. S. AL-Abadi^{2*}, and O. Sh. Dautov³

¹University of Diyala, Iraq; dhuhah_gh@yahoo.com

²University of Diyala, Iraq; msmhhjk@yahoo.com

³Kazan National Research Technical University, Russia; dautov_kstu@mail.ru

*Correspondence: M. S. AL-Abadi, Email: msmhhjk@yahoo.com

ABSTRACT- The continuous demand of sending/receiving various multimedia leads to develop 5G communications services. The 5G services requires wide bandwidth, higher speed with less time delay and all that need to use higher frequency waves that are millimeter waves. To achieve these requirements investigated a dual-band E-shape patch antenna designed on the defected ground structure (DGS) layer for 28.4/36 GHz frequency bands that are available to 5G applications. The resulted response of this antenna gives reflection factor (return loss S11) in depth of -20/-25.3dB for lower and upper frequency bands respectively. Moreover, not suffered spurious harmonics in out-of-band rejection. There is a high isolation between the two bands (about 0.2 dB). The less mismatch coincides with acceptable peak gain (3.7/1.6 dB), valuable VSWR (1.2/1.3) and high radiation efficiency (90%/84%). Furthermore, the new equivalent antenna circuit with a novel RLC configuration produces a highly consistent reflective response with the EM antenna model. In addition, the overall structure of the proposed antenna achieved in compact size less than 16 mm² to serve most of the devices in 5G systems.

Keywords: Millimeter waves, 5G, E-shape patch, Defected Ground Structure (DGS).

ARTICLE INFORMATION

Author(s): D. Gh. Hammood, M. S. AL-Abadi, and O. Sh. Dautov;

Received: 29/05/2025; **Accepted:** 22/09/2025; **Published:** 10/12/2025;
E-ISSN: 2347-470X;

Paper Id: IJEER 2905-14;
Citation: 10.37391/ijeer.130415



Webpage-link:
<https://ijeer.forexjournal.co.in/archive/volume-13/ijeer-130414.html>

Publisher's Note: FOREX Publication stays neutral with regard to jurisdictional claims in Published maps and institutional affiliations.

design. So, to ensure low-cost antenna design, have been suggested dual-band antenna as the listed work in [1-10].

In [1], a circular patch antenna printed on the top side of the defected ground to introduce dual-band at 28/38 GHz utilizing mm Waves with circuit size about 52 mm². While in [2], the stub-loaded added to the slotted rectangular patch antenna to generate the dual-band of the frequency. An antenna fabricated in large size, to a certain extent, about 1225 mm² with valuable gain 4.02/3.38 dB at 3.532/6.835 GHz. Another technique for a dual-band leaky-wave antenna used in [3], which is based on the SIW complicated structure etched on the top side of the first layer. The patch antenna inserted in array of microstrip grid and feeding with differential structure to present dual-band of the frequency at 28/38 GHz with 896 mm² complete circuit size [4]. On the other hand, the microstrip array resonating at mm waves connected through thin line feeder with pair patches at each side resonating at lower frequency band [5]. By using multilayered construction, a parasitic patch for E-band inserted in Ka-band array printed in the top layer and E-band network driven in the bottom layer and both layers coupled through grounded middle layer [6]. In contrast, based on the harmonics of the resonator a simple rectangular patch used to give dual-band resonance utilizing the multilayered construction [7]. The triple rectangular stubs and single triangular stub loaded the patch to introduce dual-band antenna resonating at 28/38GHz [8]. Moreover, the data transfer, data throughput and the gain of the multiband antenna can be rising by MIMO formation [9]. A pair of circular patch antenna with etched doughnut slot used to give 2x2 MIMO

1. INTRODUCTION

The last rising growth in the cellular communication systems involves high data rate, large capacity, and wide bandwidth to apply the multiple information between the users during short time. This demand tended to update generation of the communication in general and update the fifth generation (5G) in particular, which is expanded successfully with high frequency waves like the millimeter waves (mm Waves).

The mm Waves introduce reliable, secure, fast, and directed transmission data along wide bandwidth for frequencies more than 24 GHz. The characteristics of the mm Waves made it very desirable in many applications such as the radar, sensing components, and IOT devices. The basic component in 5G mm Waves is the antenna which is became in the light zone for the researchers that are looking for inexpensive, compact antenna

antenna resonating at 28.08/ 45.54 GHz with peak gain as 7.67/4.94dB and large size of 108 mm² [10].

As is known, microstrip antennas can support cavity resonances, much like spherical/cylindrical slotted do with the patch acting as a cavity [11, 12].

In addition, spherical conformal microstrip antennas are a bridge between the two-combining microstrip feed with spherical form factors (used on helmets, missiles, drones). In [13], The size of an antenna is 780 mm². The first resonant frequency is 5.76 GHz, and the second resonance is 26 GHz. While in [14], antenna has a gain of 7.84 dBi at the lower frequency and 7.9 dBi at the higher frequency with size of 36.72 mm². In [15], the peak gains of a millimeter-wave antenna based on microstrip dual-loop antennas and microstrip patch antennas is 8.2 dBi at 27 GHz and 9.6 dBi at 38 GHz respectively. A dual-band microstrip patch antenna with a rectangular slot etched into a rectangular patch and a half-ring slot is designed in [16]. This antenna provides gains of 3.59 dBi and 6.68 dBi at 27.68 and 34.64 GHz. The return loss in range of -46.39 dB to -28.14 dB. In [17], integrated four rectangular slots and a single circular slot in dimensions of 62 mm². The gains of 5.87 dBi and 5.404 dBi and the return losses is -36.45 dB and -22.81 dB. While in [18], gain varying from 3.8 dBi to 4.3 dBi. with a radiation efficiency of 61%.

Generally, most discussed papers are suffering large, occupied area with complicated structures in some works and that compatible with 5G systems, in principle, and that based mm Waves, especially.

In this paper a dual-band antenna based on the E-shape patch structure with defected ground is presented. Where the defected ground structure (DGS) is the popular technique used to give additional resonance frequency, enhance impedance bandwidth, minimize the attenuation and other functions. The designed work produced two bands (28.4/36 GHz) to serve the current revolution of the 5G application based on mm Waves. The first band generated by the E-Shape structure and the second band due to the $\lambda/2$ inserted slot in the ground layer by scientific calculations appropriated with 36 GHz.

The presented design analyzed and simulated with HFSS simulator in term of the VSWR, gain, directivity, reflection coefficient and radiation pattern to behave good and acceptable values at each term. The final structure designed with USA Roger (RO3010) (h = 0.64 mm) substrate in small circuit size less than 16mm².

2. E-SHAPE PATCH ANTENNA DESIGN

To cover millimeter waves, a type presented of microstrip patch antenna consists of two slots inserting in the patch *fig. 1(a)* and inserting $\lambda/2$ rectangular slot in the ground layer *fig. 1(b)*. Take in consideration the 50Ω feed line input is in the centre of the overall patch structure.

The basic parameters of an antenna [20, 21]:

$$L = L_{\text{eff}} - 2\Delta L \quad (1)$$

$$L_{\text{eff}} = \frac{c}{2f_r\sqrt{\epsilon_{\text{eff}}}} \quad (2)$$

$$\epsilon_{\text{eff}} = \frac{\epsilon_r+1}{2} + \frac{\epsilon_r-1}{2} \left[1 + \frac{12h}{w} \right]^{-1/2} \quad (3)$$

$$\Delta L = 0.41h((\epsilon_{\text{eff}} + 0.3)(\epsilon_{\text{eff}} + 0.258)^{-1}) * \left(\frac{w}{h} + 0.264 \right) \left(\frac{w}{h} + 0.8 \right)^{-1} \quad (4)$$

$$W_p = \frac{c}{2f_r\sqrt{\frac{\epsilon_r+1}{2}}} \quad (5)$$

Where, c : speed of light, f_r : resonant frequency, L , W_p : length and width of the patch respectively, L_{eff} : effective length of the patch that should be subtracted from the additional length of the fringing effect (ΔL), and ϵ_{eff} , ϵ_r , h are the effective dielectric, relative dielectric and height of the substrate respectively.

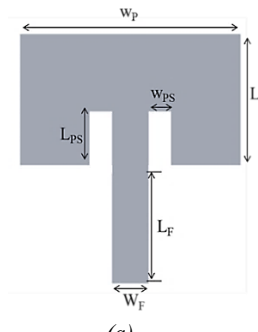
To get the compact size of the designed antenna, we configure the traditional patch antenna to E-shape patch antenna. In addition, E-shape patch antenna increases the matching, bandwidth, and selectivity at the desired frequencies (f_1, f_2). The construction of E-shape patch antenna is formed by etching two $\lambda/4$ slots around the input feed line according the following equation [20, 22]:

$$L_{\text{slot}} = \frac{c}{2f_{\text{slot}}\sqrt{\frac{\epsilon_r+1}{2}}} \quad (6)$$

where, L_{slot} is the physical length of the structure.

Since the E-shape has a specific or confined current distribution within a smaller area, the coupling between the side arms (open-circuit end) and the middle arm (short-circuit end) is increased, thus contributing to the second band being clearly visible, forming a dual-band antenna. To get more matching and good isolation between the two bands the defected ground is utilized as shown in *fig. 1(b)*, where the $\lambda/2$ etched ground slot in compatibility with the second frequency band. This slot increased the matching for the first frequency band (28.4 GHz) and contributed to shift the second band to the desired frequency (38GHz).

Furthermore, the defected ground indicated by $\lambda/2$ slot also allowed minimizing the overall designed structure of the antenna in compatible way with the $\lambda/4$ patch slots. That leaded to decrease the expected radiation from the microstrip structure at the edge and showed good flatness at the stop bands [23], [24].



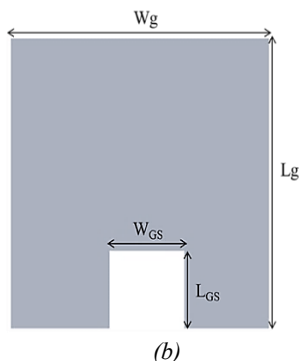


Figure 1. The structure of E-patch antenna. (a) Top Layer (b) Ground Layer

The overall structure of the antenna built with Roger substrate (RO3010) which has thickness about 1.64 mm and 10.2 relative dielectric. The analysing steps accomplished by using Ansys HFSS simulator version 14 [25]. Due to the defected ground, the overall dimensions of the antenna had been tuned and optimized after inserting in HFSS and that enhanced the results. The final dimensions of the designed antenna shown in the *table 1*.

Table 1. Dimensions of the E-patch antenna structure

Antenna dimensions	Label	Value (mm)
Ground Length	L _g	3.5
Ground Width	W _g	4.5
Ground Slot Length	L _{GS}	1.19
Ground Slot Width	W _{GS}	1.15
E-Patch Length	L _P	1.6
E-Patch Width	W _P	3.26
Feeder Length	L _F	0.95
Feeder Width	W _F	0.5
Patch Slot Length	L _{PS}	0.68
Patch Slot Width	W _{PS}	0.3

3. ANALYSIS OF THE EQUIVALENT CIRCUIT

As it is known, the microstrip components are distributed elements and the equivalent circuit of the components can be formed using the passive elements (R, L, C). For high compatible reflection response with EM model of the antenna new configuration of the lumped equivalent circuit introduced as shown in *fig. 2 (a)*. The E-patch equivalent circuit is two RLC resonators capacitively coupled. The first (R₁, L₁, C₁) resonator represents the middle stub that has straight path of the current. The second (R₂, L₂, C₂) resonator of the edge stub which has longer path of the current introduces a new inductance (ΔL) plus the additional capacitance (ΔC) due to the slots effect. In this paper, the DGS layer represented by parallel (L₃, C₃) resonator with series (R₃, C₄) circuit due to the dielectric material of the substrate. The Keysight ADS ver.11 [26] used to simulate the overall equivalent circuit *fig. 2(a)* and the reflection coefficient (S₁₁) results viewed high

compatibility with the electromagnetic simulation of the E-Patch by HFSS as shown in *fig. 2(b)*.

The passive elements values of the circuit that achieved by ADS as following: R₁=2.28K Ω , L₁=0.34nH, C₁=2.64PF, R₂=527K Ω , L₂=0.06nH, C₂=0.02PF, ΔL =0.42nH, ΔC =0.06PF, L₃=0.5nH, C₃=0.11PF, R₃=5.7K Ω , C₄=0.05PF, C₁₁=0.6PF, C₂₂=0.4PF, C₃₃=0.05PF.

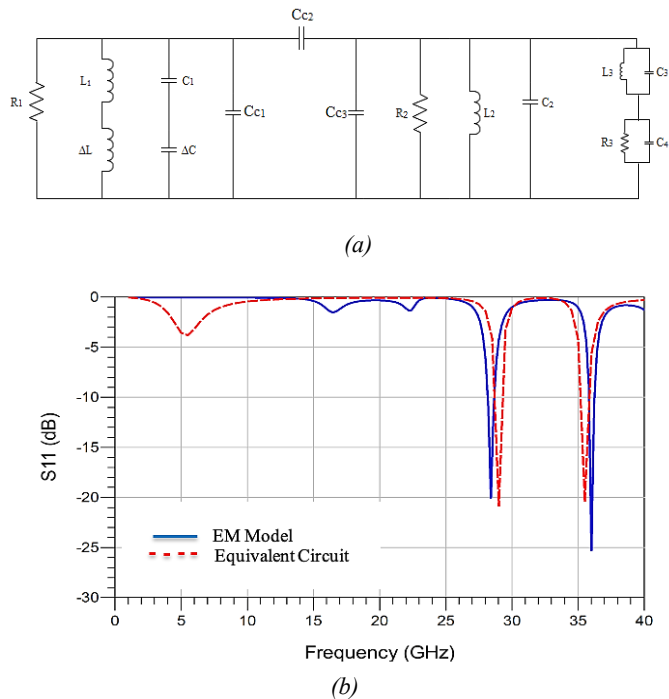


Figure 2. (a) Lumped equivalent circuit of the proposed antenna (b) Reflection coefficients for EM model and the lumped equivalent circuit

Another representation equivalent circuit of the designed E-Patch can be presented using even-odd mode analysis due to symmetrical effect [27, 28]. The odd mode *fig. 3(a)* represents the higher frequency band according to the *equation (6)*. The even mode *fig. 3(b)* represents the lower frequency band as indicated in *equation (8)*.

$$f_{\text{odd}} = \frac{c}{(l_1 + l_2) \sqrt{\epsilon_{\text{eff}}}} \quad (7)$$

$$f_{\text{odd}} = \frac{c}{2(l_3 + l_4) \sqrt{\epsilon_{\text{eff}}}} \quad (8)$$

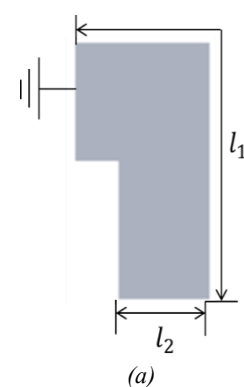




Figure 3. Odd-Even analysis of the designed E-patch antenna (a) Odd mode (b) Even mode

4. RESULTS AND DISCUSSION

The designed E-Shape antenna simulated by Ansys HFSS simulator in free space for mmWave frequencies. Return loss is a critical metric that reflects how effectively an antenna is aligned with the transmission line or source. A high backlash loss (*i.e.*, more negative in decibels) indicates low reflected power and low power transfer efficiency. In this graph (*figure 4*), the backlash loss is expected to show sharp notches (deep dips) at resonant frequencies, such as 28.4 GHz and 36 GHz. These minimum values confirm that the antenna is resonant and well aligned in the desired operating bands, which is essential for minimal reflection and optimal power savings. Thus, we observe a good match in both bands. The lower rejection bands came with long range flatness (from 0-26 GHz) that characterizes the reflection plot as shown in *fig. 4*. In addition, the return loss showed high selectivity and pure flatness between the two bands. The return loss for the first/second bands about 20/25 dB. Such that with bandwidth about 300MHz, at the lower band (28.4GHz) and 250MHz at the higher band (36GHz).



Figure 4. Return loss against frequency

As for the VSWR, the VSWR presented with less mismatch at the desired frequencies and that indicate good matching between the input feeding and the patch. The plotted VSWR (*fig. 5*) showed valuable results, where at the first band up to 1.2 and 1.3 at the second band. The achieved VSWR at the designed mmWave frequencies refer to, the proposed antenna can be fabricated with compatible measurements at the dual bands.

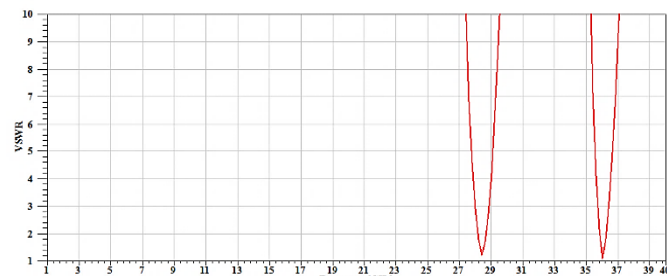
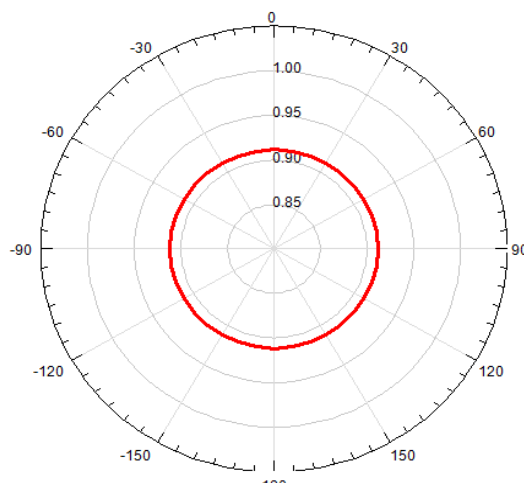
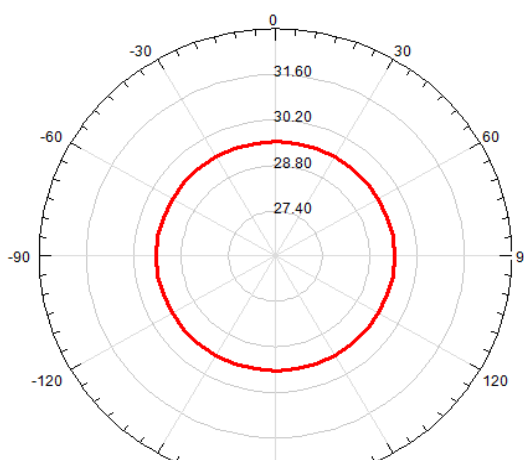


Figure 5. VSWR against frequency

Another significant parameter of the proposed antenna is antenna radiation efficiency that shown in *fig. 6 (a)*. Such that, the value of the red circle on the y-axis represents the value of radiation efficiency with respect to θ -angle. It is 91% at the operating frequencies. At the same time, the radiated power of the analyzed E-patch antenna is about 29.5 dBm as shown in *figure 6 (b)*.



(a)



(b)

Figure 6. (a) The value of antenna radiation efficiency with respect to θ -angle (b) The value of antenna radiated power with respect to θ -angle

Taken in consideration the 2D plot, *fig. 7*, was 3.7dB/1.6dB at the first/second band respectively. However, high frequencies have less gain compared to low frequencies. This is evident in *fig. 7*, where the gain decreases in the upper band of frequency (36GHz) compared to frequency (28.4GHz). The overall gain of the proposed antenna which is presented in 3D plot *fig. 8* raising up to 3.5dB. *Figure 9* shows the simulated 3D total directivity.

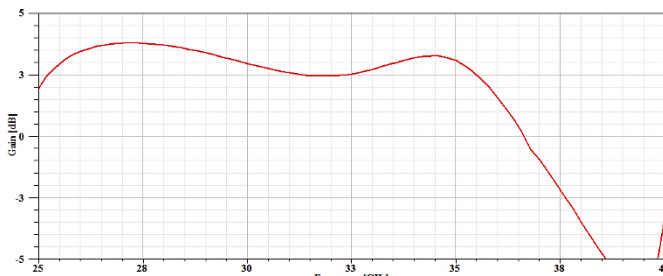


Figure 7. The 2D simulated gain for desired frequencies

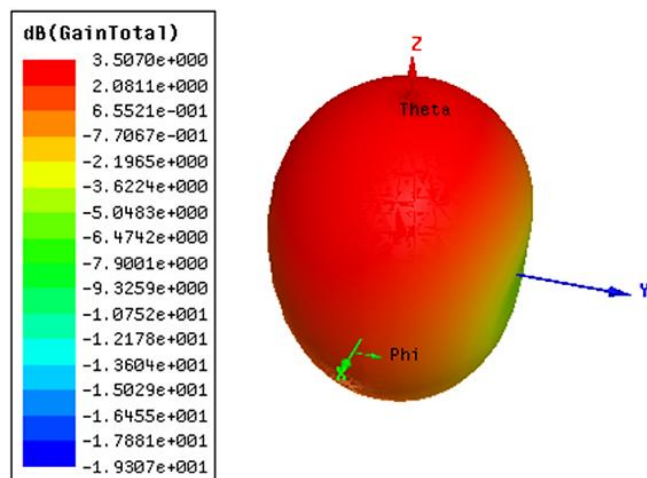


Figure 8. The 3D simulated gain for desired frequencies

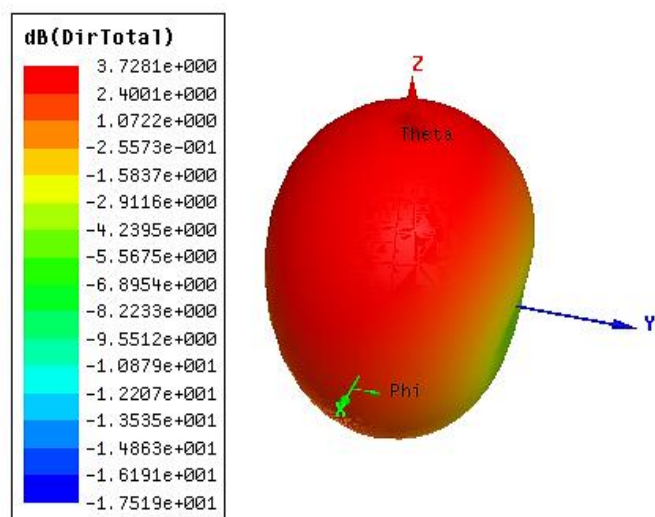


Figure 9. The simulated 3D total directivity

The surface current distribution (Amper/meter) of the proposed patch antenna, shown in *figure 10*, is affected by DGS in both bands. In *fig. 10*, at lower band (28.4GHz), the current has been increased strongly at the edges of the E-patch and the feed line. In other side, at the higher frequency band (36GHz) the central edge of the E-patch is activated with higher surface current than the edge as shown in *fig. 11*.

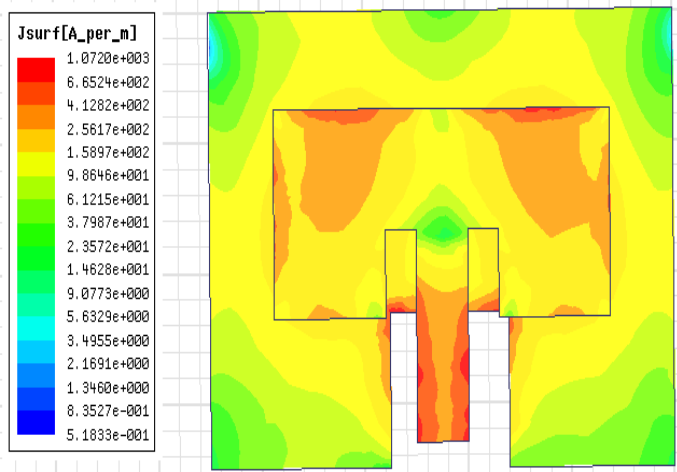


Figure 10. The surface current distribution at 28.4GHz

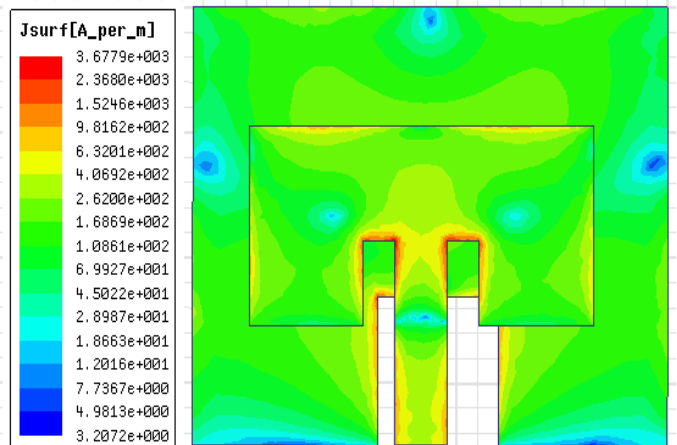


Figure 11. The surface current distribution at 36GHz

As it is known, in antenna theory, cross-polarization refers to the unwanted radiation or reception of an electromagnetic wave with a polarization perpendicular to the intended polarization. While an antenna, ideally, transmits or receives only in its intended, or co-polarization, direction, realistic constraints cause some energy to be radiated or received in the perpendicular, or cross-polarization, direction. High cross-polarization is undesirable because it can lead to signal interference and reduce the capacity of communication links. However, *figure 12* shows the co- and cross- polarized beam patterns for the proposed antenna. The radiation patterns show good patch type radiation for the E-planes with good cross polar discrimination of at least -18 dB in $\phi \pm 90^\circ$.

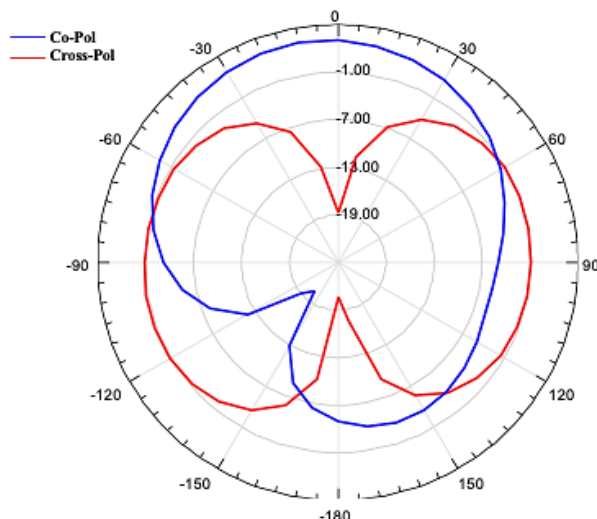


Figure 12. Co-polarized and cross polarized radiation patterns

Finally, the table below (*Table 2*) shows a comparison between our research and the last works that were selected for last different years. It is clear that the proposed antenna gives high radiation efficiency and it has very acceptable VSWR. Moreover, the proposed antenna has acceptable gain despite it has very small size compared to previous works. This gain can be made even greater using adaptive beamforming. In addition, it is possible to increase the gain for this antenna by using this antenna as a phased array antennas in our future work.

Table 2. Comparison between the present work and the last works

Refer ences	Freque nacy (GHz)	Size (mm ²)	Gain	S11 (dB)	SWR	Rad eff (%)
[1]	28/38	52.27	6.87/4.17 dB	-27/-15	-	90
[2]	28/38	1122	4.02/3.38 dB	-45/-15	-	88.2
[12]	37.45/3 9.8	36.7	7.84/7.9 dBi	- 47.82	-	-
[14]	27.68/3 4.64	-	3.59/6.68 dBi	-46.39/ -28.14	1.08/1 .009	-
[15]	28/37	62	5.87/5.40 dBi	- 36.45/- 22.81	-	-
[17]	28	-	8.2 dB	-38.34	1.0244	77
Present work	28.4/36	16	3.7dB/1.6 dB	-20/-25	1.2/1.3	91

5. CONCLUSION

This paper offered dual-band E-shape patch antenna with defected ground layer. The simulated parameters of the presented E-patch antenna have produced valuable results in terms of reflection, VSWR, gain and directivity when compared to the state-of-the-art research. Subsequently, the lumped element circuit has yielded full operation match with electromagnetic simulation. It is worth noting that, the overall presented structure of the proposed antenna has been constructed with less than 16mm² circuit size and many features that make it a very suitable antenna for 5G system applications. It is worth noting also that the small dimensions of this antenna (3.5 mm × 4.5 mm) can be used also in a capsule in medical applications for the purpose of conducting medical checks.

Conflicts of Interest: The authors declare no conflict of interest.

Funding: This research received no external funding.

REFERENCES

- [1] A. QAYYUM; A. H. Khan; S. Uddin; O. Ahmad; J. S. Khan; S. Bashir Abdullah, A novel mmwave defected ground structure based Microstrip antenna for 5G cellular application, 2020 First International Conference of Smart Systems and Emerging Technologies (SMARTTECH), IEEE, Riyadh, Saudi Arabia, 2020, p. 28-31. <https://doi.org/10.1109/SMARTTECH49988.2020.00023>
- [2] M. M. Rahman, M. S. Islam, H. Y. Wong, T. Alam, M. T. Islam, Performance analysis of a defected ground-structured antenna loaded with stub-slot for 5G communication, *Sensores*, 2019, vol. 19, p. 2634. <http://dx.doi.org/10.3390/s19112634>
- [3] Y. Li; J. Wang, Dual-band leaky-wave antenna based on dual-mode composite microstrip line for microwave and millimeter-wave applications, *IEEE Transactions on Antennas and Propagation*, 2018, vol. 66, p. 1660-1668. <https://doi.org/10.1109/TAP.2018.2800705>
- [4] G. Xu; L. X. Yang; Z. X. Huang; W. Wang; H. L. Peng; Y. Zhang; W. Y. Yin, Microstrip grid and patch-based dual-band shared-aperture differentially fed array antenna, *IEEE Antennas and Wireless Propagation Letters*, 2021, vol. 20, p. 1043-1047. <https://doi.org/10.1109/LAWP.2021.3070219>
- [5] Y. Q. Guo; Y. M. Pan; S. Y. Zheng, A singly-fed dual-band microstrip antenna for microwave and millimeter-wave applications in 5G wireless communication, *Transactions on Vehicular Technology*, 2021, vol. 70, p. 5419-5430. <https://doi.org/10.1109/TVT.2021.3070807>
- [6] M. S. Elsayed; M. F. A. Sree; M. H. Abd Elazeem, A dual band rectangular patch antenna for 5G applications12 2020, th International Conference on Electrical Engineering (ICEENG), IEEE, Cairo, Egypt, 2020, p. 200-202. <https://doi.org/10.1109/ICEENG45378.2020.9171733>
- [7] Z. Wang; Z. Huang, A microwave/millimeter wave dual-band shared aperture patch antenna array, *IEEE Access*, 2020, vol. 20, p. 218585 – 218591. <https://doi.org/10.1109/ACCESS.2020.3040250>
- [8] R. Sabek; A. A. Ibrahim; W. A. Ali, Dual-band millimeter wave microstrip patch antenna with Stub Resonators for 28/38 GHz applications, *Journal of Physics :Conference Series* IOP Publishing, 2006, vol. 2128, p. 1-10. <http://dx.doi.org/10.1088/1742-6596/2128/1/012006>
- [9] M. N. Hasan; S. Chu; S. Bashir, A DGS monopole antenna loaded with U-shape stub for UWB MIMO applications, *Microwave and optical technology letters*, 2019, vol. 61, p. 2141-2149.
- [10] G. M. Amrutha; T. Sudha, Millimeter wave doughnut slot MIMO antenna for 5G applications2019, IEEE Region 10 Conference (TENCON), Kochi, India, 2019, p. 1220-1224. <https://doi.org/10.1109/TENCON.2019.8929658>
- [11] Q. Xu et al., A Compact Dual-band Microstrip Patch Antenna for 5G Applications, 2022 IEEE MTT-S International Microwave Biomedical Conference (IMBioC), Suzhou, China, 2022, p. 223-225. <https://doi.org/10.1109/IMBioC52515.2022.9790193>



© 2025 by D. Gh. Hammood, M. S. AL-Abadi, and O. Sh. Dautov. Submitted for possible open access publication under the terms and conditions of the Creative Commons Attribution (CC BY) license (<http://creativecommons.org/licenses/by/4.0/>).

[12] M. A. M. Ali; A. S. A. Gaid; M. M. Saeed and R. A. Saeed, Design and Performance Analysis of a 38 GHz Microstrip Patch Antenna with Slits Loading for 5G Millimeter-Wave Communications, 2023 3rd International Conference on Emerging Smart Technologies and Applications (eSmarTA), Taiz, Yemen, 2023, p. 1-6. <https://doi.org/10.1109/eSmarTA59349.2023.10293289>

[13] Osman Shakirovich Dautov; Mohammad Sadon AL-Abadi; Haidar N. Al-Anbagi, New proposed spherical slotted antenna covered by the layers of dielectric material and plasma, International Journal of Electrical and Computer Engineering (IJECE), 2020, vol. 10, p. 1728-1735. <http://dx.doi.org/10.11591/ijece.v10i2.pp1728-1735>

[14] Al-Abadi. Mohammad. S., Hammood D. Gh., Dautov Osman Shakirovich, Shaaban Mohamed. N., Cylindrical Conformal Antenna in a Homogeneous Plasma, IIETA, 2025, p. 1849-1856, 2025. <https://doi.org/10.18280/mmep.1206>

[15] D. Huang; F. Liang; X. Wang and B. -Z. Wang, A Millimeter-Wave Dual-Band Antenna Based on Microstrip Dual-Loop and Patch, IEEE Antennas and Wireless Propagation Letters, 2024, vol. 23, no. 10, p. 2825-2829. <https://doi.org/10.1109/LAWP.2024.3408422>

[16] S. Saha; F. Sultana, M. F. Hossain; D. Das and M. A. Hossain, Modified D Shaped Dual-Band Microstrip Patch Antenna for 5G Ka Band Application, 2024 3rd International Conference on Advancement in Electrical and Electronic Engineering (ICAEEE), Gazipur, Bangladesh, 2024, p. 1-5. <https://doi.org/10.1109/ICAEEE62219.2024.10561691>

[17] M. F. H. Mihad; H. Kawsari; R. Parveen; H. Rani and M. Rahman, A Slotted Patch Antenna for 5G Applications Operating at 28 GHz and 37 GHz, 2024 3rd International Conference on Advancement in Electrical and Electronic Engineering (ICAEEE), Gazipur, Bangladesh, 2024, p. 1-5. <https://doi.org/10.1109/ICAEEE62219.2024.10561733>

[18] M. H. Akash and M. Saito, Low Profile Single/Two-Element Dual-Band Array Antenna for 5th Generation Mobile Communications, 2024 IEEE International Symposium on Antennas and Propagation and INC/USNC-URSI Radio Science Meeting (AP-S/INC-USNC-URSI), Firenze, Italy, 2024, p. 1657-1658. <https://doi.org/10.1109/AP-S/INC-USNC-URSI52054.2024.10686238>

[19] Md. Sohel Rana; Md. Mostafizur Rahman Smieee., Design and analysis of microstrip patch antenna for 5G wireless communication systems, Bulletin of Electrical Engineering and Informatics, 2022, p. 3329~3337. <https://doi.org/10.11591/eei.v11i6.3955>

[20] C. A. Balanis, Antenna Theory: analysis and design (Wiley, Fourth Edition).

[21] Muhammad Irfan Khattak, Muhammad Irshad Khan, Zaka Ullah, Gulzar Ahmad, and Amad Khan, Hexagonal Printed Monopole Antenna with Triple Stop Bands for UWB Applications, Mehran University Research Journal of Engineering & Technology, Vol. 38, No. 2, p. 335-340, 2019

[22] R. Garg, "Microstrip antenna design handbook, (Artech house2001,).

[23] O. S. Dautov and M. S. Al-abadi, the optimal excitation voltage for spherical slotted antenna coated by two layers of dielectric material and plasma, 2021 International Siberian Conference on Control and Communications (SIBCON), Kazan, Russia, 2021, p. 1-6. <https://doi.org/10.1109/SIBCON50419.2021.9438871>

[24] Vladimir Niriforovich LAVRUSHEV1; Osman Shakirovich Dautov; Mohammad Sadon Al-abadi; Ali Nadhim Jbarah Almaki, scattering of electromagnetic waves by plasma layer sandwiched between two layers of thin glass.,//Przeglad Electrotechniczny, 2023, vol. 99, no. 4, p. 102-107. <https://doi.org/10.1109/SIBCON50419.2021.9438871>

[25] Ansys HFSS simulator version 14.

[26] The Keysight ADS ver.11

[27] F. Yang; X. X. Zhang; X. Ye; Y. Rahmat-Samii, Wide-band E-shaped patch antennas for wireless communications, IEEE transactions on antennas and propagation, 2001, vol. 49, p. 1094-1100. <https://doi.org/10.1109/8.933489>

[28] D. G. Hammood; R. T. Hammed, Performance Enhancement of Miniaturized Dual-Band Bandpass Filter, IOP Conference Series: Materials Science and Engineering, 2021, vol. 1076, p. 1-9. <http://dx.doi.org/10.1088/1757-899X/1076/1/012049>